

## GREEN SYNTHESIS OF CUO NANOPARTICLES FOR THE APPLICATION OF DYE SENSITIZED SOLAR CELL

Worku Wubet Andualem\*<sup>1</sup>

Department of Chemistry College of Natural Sciences, Arba Minch University, Ethiopia.

Article Received on  
27 August 2020,

Revised on 17 Sept. 2020,  
Accepted on 07 Oct. 2020

DOI: 10.20959/wjpr202013-18436

### \*Corresponding Author

Worku Wubet Andualem

Department of Chemistry  
College of Natural Sciences,  
Arba Minch University,  
Ethiopia.

### ABSTRACT

*In recent years, the development of efficient green chemistry methods for synthesis of metal oxide nanoparticles has become a major focus of researchers. The investigations carried out are in an attempt to find an eco-friendly technique for the production of well-characterized nanoparticles. One of the most considered methods is production of metal oxide nanoparticles using cost efficient and environment favoring methods like green synthesis. A review with the perspective of synthesis of Copper oxide nanoparticles have been presented here. Synthesis of high-quality nanoparticles with respect to chemical purity, phase selectivity, crystallinity and homogeneity in particle size with*

*controlled state of agglomeration in a cost-effective procedure is still a challenge to material chemists. Consequently, many efforts have been devoted to the finding of sustainable reactions from the feedstocks to solvents, to synthesis and to processing. Green chemistry actively seeks ways to produce materials in a way that is more benign to human health and the environment. It encompasses a series of considerations in the design of environmentally benign protocols. A major point in the design of greener and more sustainable processes relates to the efficiency of the process, which has to take into account several parameters including energy, material consumption (preferably use of bio-renewable resources) and man-power. The synthesized copper oxide nanoparticles are characterized by Fourier transformed infrared spectroscopy (FTIR) to identify functional groups, and scanning electron microscopy (SEM) to characterize nanoparticles size and morphology, UV-Vis spectroscopy to characterize optical properties of CuO nanoparticles and X-ray powder to characterize crystal structure. CuO NPs in dye sensitized solar cell used as counter electrode. Natural dyes are environmentally and economically superior to ruthenium-based*

*dyes because they are nontoxic, cheap, easy attainability and abundance in supply of raw materials.*

**KEYWORDS:** Nanoparticles, CuO, DSSCs, Counter electrode.

## INTRODUCTION

Nanotechnology is an intensive branch of science that deals with materials among the size of 1-100 nm with different shapes of spherical nanoparticles, nanorods, nanoribbons, nanobelts and nanoplatelets. The unique physical and chemical properties are due to its high surface-to-volume ratio comparing with micro or bulk-sized. Nanomaterials are now become available and useful in all the man daily life applications such as in: medicine, solar cells, water purification, pharmaceutical and catalysts.<sup>[1]</sup>

Nanomaterials are classified into nanostructured materials and nanophase/nanoparticle materials. The former refer to condensed bulk materials that are made of grains with grain sizes in the nanometer size range while the latter are usually the dispersive nanoparticles. To distinguish nanomaterials from bulk, it is vitally important to demonstrate the unique properties of nanomaterials and their prospective impacts in science and technology.<sup>[2]</sup>

Nanomaterials have properties that are significantly different and considerably improved relative to those of their coarser-grained counterparts. The property changes result from their small grain sizes, the large percentage of their atoms in large grain boundary environments and the interaction between the grains. Research on a variety of chemical, mechanical and physical properties is beginning to yield a glimmer of understanding of just how this interplay manifests itself in the properties of these new materials. In general, one can have nanoparticles of metals, semiconductors, dielectrics, magnetic materials, polymers or other organic compounds. Semiconductor heterostructures are usually referred to as one-dimensional artificially structured materials composed of layers of different phases/compositions. The semiconductor heterostructured material is the optimum candidate for fabricating electronic and photonic nanodevices.<sup>[3]</sup>

## Synthesis Methods of Copper Oxide Nanoparticles

Nanoparticles can be formed by two approaches: top-down (comminution and dispersion) or bottom-up (nucleation and growth).<sup>[4]</sup> Top-down approach is making use of the starting bulk materials of the same materials that going to be synthesized and applying energy to break

down the large materials into smaller fragments. Sources of energy can be mechanical, thermal or chemical. However, there is a disadvantage associated with this method whereby this will be creating particles with wide size distribution. To overcome this, bottom-up method was introduced as it is considered simpler and more favorable in synthesizing nanoparticles in size less than 100 nm whereby it was like building the atoms one by one, first started with a simple metal salt, slowly converts it from ions to elemental atoms by chemically eventually clumped and grown in the form of nano-size particles.<sup>[4]</sup>

CuO NPs can be synthesized by various chemical methods such as sol-gel method, precipitation, hydrothermal synthesis, chemical reduction, thermal decomposition, electrochemical method and wet chemical method. Conventional chemical methods for nanoparticles synthesis are associated with various disadvantages such as expensive, involve the use of chemicals, time consuming and pose environmental threats by generating toxic solvent and waste products<sup>[5]</sup> which leads to a growing need to develop greener, environmentally friendly approach in synthesizing the metal nanoparticles. It has been reported that many of the biological systems such as bacteria, fungi, algae, plants and human cells can be used to convert metal ions into metal nanoparticles.<sup>[6]</sup>

### **Green Synthesis of CuO Nanoparticles**

According to the 12 principles of green chemistry, synthesis of nanoparticles by using plant extract and microorganism has an advantage over conventional methods.<sup>[7]</sup> This approach provides a safer alternative to produce nanoparticles with desired physical and chemical properties. However, there are certain limitations to be taken note of during synthesis part as different synthesis methods could give different types of nanoparticles. Firstly, the size and shape of nanoparticles formed depends on the types of green synthesizer used, different amount of extract used, experiment parameters and these factors could lead to subsequent changes in nucleation process and number of functional groups deposited on the existing nanoparticles surface to avoid agglomeration.<sup>[8]</sup>

Due to the wide applications in diverse branches of advanced scientific fields, more and more researchers have been focused on the synthesis of CuO NPs in different routes. The brief review of synthesis of CuO NPs is described as below. Metal salt of corresponds metal nanoparticles going to be synthesized is chosen as the precursor in preparation of nanoparticles. They are reduced to metal ions in the presence of bioactive functional groups present in the natural sources.<sup>[9]</sup>

### **CuO Nanoparticles Synthesis Using Algae**

Algae are eukaryotic aquatic oxygenic photoautotrophs, which produces its food through photosynthesis using sunlight producing oxygen as their byproduct. Their photosynthesis machinery has been evolved from cyanobacteria via. endosymbiosis. They are predominant primary producers in many marine/aquatic environments. Among various algae, *Chlorella sp.* is found to uptake various heavy metals such as cadmium, uranium, copper, and nickel.<sup>[10]</sup>

Synthesis of nanoparticles using algae can be performed in three important steps, Firstly preparation of algal extract in water or in an organic solvent by heating or boiling it for a certain duration, Secondly preparing of molar solutions of ionic metallic compounds and lastly incubating of algal solutions and molar solutions of ionic metallic compounds followed either by continuous stirring or without stirring for a certain duration under controlled conditions.<sup>[11]</sup> The synthesis of nanoparticle is dose dependent and it is also related to the type of algae used. There are a variety of biomolecules responsible for the reduction of metals which include polysaccharides, peptides, and pigments. Stabilizing and capping the metal nanoparticles in aqueous solutions is done by proteins through aminogroups or cysteine residues and sulphated polysaccharides.<sup>[12]</sup>

The biomedical application of algal-synthesized NPs is significantly becoming more important due to their antibacterial, antifungal, anticancer, and wound healing activity. Brown alga (*Bifurcaria bifurcata*) is reported for the synthesis of copper oxide nanoparticle exhibiting antibacterial activity against *Enterobacter aerogenes* (Gram negative) and *Staphylococcus aureus* (Gram positive).<sup>[13]</sup>

### **CuO Nanoparticle Synthesis Using Fungi**

Synthesis of nanoparticles outside the cell, extracellularly, has many applications as it is void of unnecessary adjoining cellular components from the cell. Mostly, fungi are regarded as the organisms that produce nanoparticles extracellularly because of their enormous secretary components, which involve in the reduction and capping of nanoparticles. Biosynthesis of metal nanoparticles by Fungi includes easy and simple scale up method, economic viability, easy downstream processing and biomass, handling and recovery of large surface area with optimum growth of mycelia.<sup>[14]</sup>

Microorganisms such as *Fusarium oxysporum* are able to leach copper from integrated circuits present on electronic boards under ambient conditions.<sup>[15]</sup> The analysis of the

biogenic synthesis of copper oxides from  $\text{CuSO}_4$  by *Penicillium aurantiogriseum*, *P. citrinum*, *P. waksmanii*, and *F. oxysporum* showed no large polydispersity in the pH range of 5 to 9.<sup>[16]</sup> In this context, a limited number of studies have been published, and these evaluated different fungal strains for the biosynthesis of copper nanoparticles. Fungi, such as *Penicillium* sp. and *F. oxysporum* strains, have been reported to biosynthesize copper oxide and  $\text{Cu}_2\text{S}$  nanoparticles.<sup>[16]</sup>

The synthesis of copper or copper oxide nanoparticles can present different surface plasmon resonance, formed by the strong coupling between incident electromagnetic radiation and surface plasmons in metal nanoparticles.<sup>[17]</sup> The use of copper or copper derivatives for the biosynthesis of nanoparticles using fungal strains has only been reported using  $\text{CuSO}_4$  copper salt, and no comparative studies have been performed using other copper salts, such as  $\text{CuCl}_2$  or  $\text{Cu}(\text{NO}_3)_2$ , with other fungal strains. Moreover, it is important to note that the biosynthesis of metal nanoparticles using different fungal extracts is really clean and environmentally friendly.<sup>[16]</sup> In addition, metals such as copper and biosynthesized copper nanoparticles have been shown to have better antimicrobial activity than nanoparticles synthesized via synthetic routes.<sup>[18]</sup>

### **CuO Nanoparticles Synthesis Using Bacteria**

In green nanotechnology, different microorganisms produce inorganic materials, either intracellularly or extracellularly with properties similar to chemically synthesized materials.<sup>[19]</sup> Usha *et al.* reported a green synthesis of copper oxide by *Streptomyces* Sp for development of antimicrobial textiles which can be useful in hospitals to prevent or to minimize infection with pathogenic bacteria. For development of antimicrobial textiles which can be useful in hospitals to prevent or to minimize infection with pathogenic bacteria. Singh *et al.*<sup>[21]</sup> reported biological synthesis of copper oxide nanoparticles using *Escherichia coli* with a variable size and shapes for antibacterial activity.<sup>[20]</sup>

### **CuO Nanoparticles Synthesis Using plant Extract**

Phytonanotechnology has become an upcoming new area of research for biological synthesizing method of metal nanoparticles. Plant extract is far more advantageous with the present of functional components in plants which can be used as a reducing agent and capping agent as well. This is a better method as they give excellent manipulation on controlling the particle size growth thus provide considerably stabilization during synthesizing process.<sup>[22]</sup> By making use of plant extract, specific nanoparticles with desired

size and shape can be designed for wide variety of nanotechnological applications. Various parts of the plants can be used for synthesis of metal nanoparticles including leaves, stems, roots and seeds. It has been reported that the phytochemicals, primary and secondary metabolites are well known as natural resources that responsible for metal salt reduction.<sup>[23]</sup> The degree of accumulation of metal nanoparticles is influenced by the reducing power of the plant extract with the reacting metal ion's oxidation state. Figure 1 shows the process of synthesis and characterization of nanoparticles.

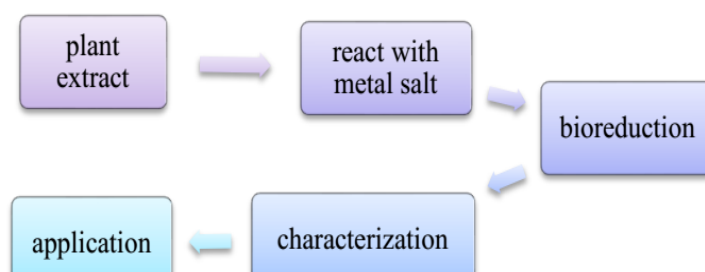


**Figure 1: Flow Chart of Nanoparticles Synthetic Pathway Using Plant as Green Source.**<sup>[23]</sup>

Naika *et al.* reported the synthesis of copper oxide nanoparticles by using *Gloriosa superba* L. for photocatalytic activity.<sup>[24]</sup> Another research by Jayalakshmi and Yogamoorthi, they are using flower of *Cassia alata* to synthesis CuO NPs, *Cassia alata* L. is belong to family Fabaceae which reported to have phytochemical activity.<sup>[25]</sup> *Cassia alata* has been analyzed to contain active anthraquinones such as rhein, emodin, physcion and flavonoid a photocatalytic activity.<sup>[26]</sup>

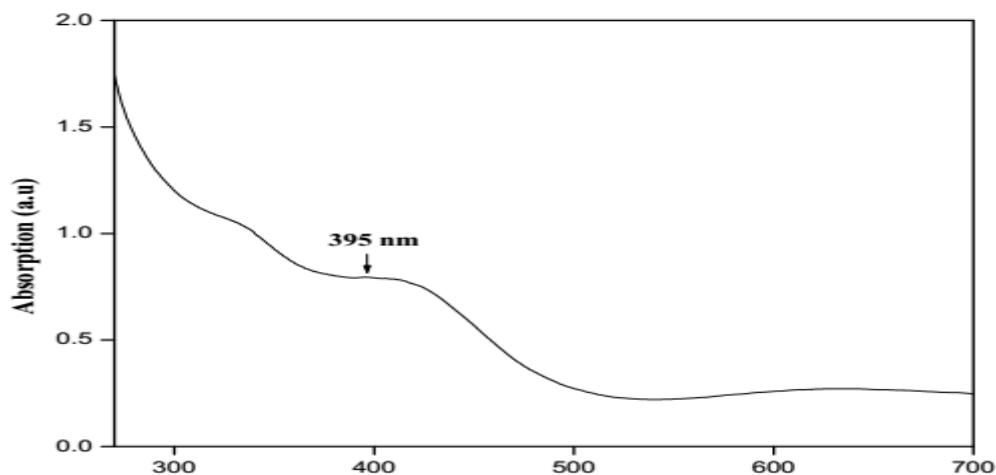
### Characterization Methods of CuO Nanoparticles

#### UV-Vis Spectroscopy Analysis

UV-VIS Spectroscopy deals with the recording of absorption signals due to electronic transitions. In semiconductors, when the incident photon energy exceeds the band gap energy of the materials, absorption takes place and signal is recorded by the spectrometer whereas in metals when the surface free electrons vibrate coherently with the incident frequency then resonant absorption takes place.<sup>[27]</sup>

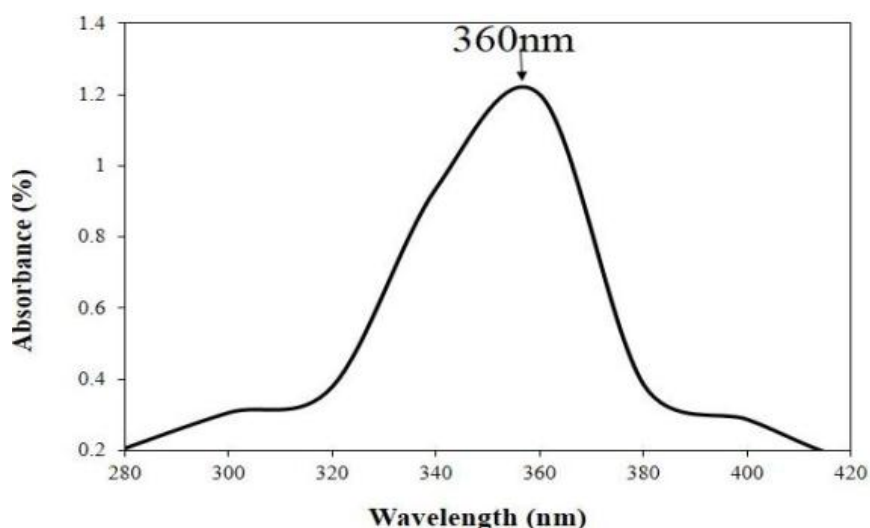
Such a spectrometer can operate in two modes that are transmission and reflection mode. In transmission mode usually thin films and colloidal NPs well-dispersed in solvent are used. The optical measurements for opaque thin films and those NPs which are not dispersible in solvents are done in diffuse reflectance (DRS) mode.<sup>[27]</sup>

Figure 2 depicts the UV–Vis spectrum of biosynthesized copper oxide nanoparticles using *Puysr Pyrifolia* leaf extract. The CuO NPs is dispersed in liquid ammonia with a concentration of 0.1 wt%, sonicated for uniform dispersion of CuO Nps and so subjected for UV – visible spectrophotometric measurements. The CuO Nps exhibiting the optical absorption peak at wavelength of 395 nm.<sup>[28]</sup>



**Figure 2: Shows UV–Visible Spectra of CuO Nanoparticle Using *Puysr Pyrifolia* Leaf Extract.**<sup>[28]</sup>

Figure 3 shows the UV–Vis absorption spectrum of CuO NPs using *Ixora coccinea* leaf extract. The absorption spectrum is recorded for the sample in the range of 280–420 nm. The spectrum shows the absorbance peak at 360 nm corresponding to the characteristic band of copper oxide nanoparticles.<sup>[29]</sup>



**Figure 3: UV-visible Spectrum of Copper Oxide Nanoparticles Synthesized from *Ixora coccinea* Leaf Extract.**<sup>[29]</sup>

The band gap energy ( $E_g$ ) of the synthesized CuO nano material is obtained by using Equation 1.<sup>[30]</sup>

$$E_g = \frac{1240}{\lambda} \text{ eV.m (1)}$$

Where  $E_g$  is the band gap in electron volt (eV) and  $\lambda$  is the wave length of the absorption edges in the spectrum in nano mater (nm). The synthesized CuO NPs band gap energy is (3.14 eV) and (3.44 eV) respectively. This indicates that the band gap of the semiconductors has been found to be particle size dependent. The band gap increases with decreasing particle size and the absorption edge is shifted to a higher energy (blue shift) with decreasing particle size.<sup>[30]</sup>

### FT-IR Analysis of CuO NPs

FTIR spectroscopy analysis was carried out to find the functional groups of biomolecules that were bound specifically along the CuO NPs surface. The FTIR spectra of biosynthesized CuO NPs and leaf powder of *P. Pyrifolia* were shown in Figure 4. The spectrum depicted bands at  $528 \text{ cm}^{-1}$ ,  $669 \text{ cm}^{-1}$  are assigned to M–O stretching of CuO (M–O). The broad and strong absorption bands were  $3435 \text{ cm}^{-1}$ ,  $2362 \text{ cm}^{-1}$  corresponds to O–H stretching H–bonded alcohols, phenols, C–H stretching aldehydes.  $2924 \text{ cm}^{-1}$  C–H stretching alkanes,  $1637 \text{ cm}^{-1}$  C=O stretching and N–H bend  $1^\circ$  amines,  $1423 \text{ cm}^{-1}$ ,  $1024 \text{ cm}^{-1}$  C-O stretching.<sup>[31]</sup>

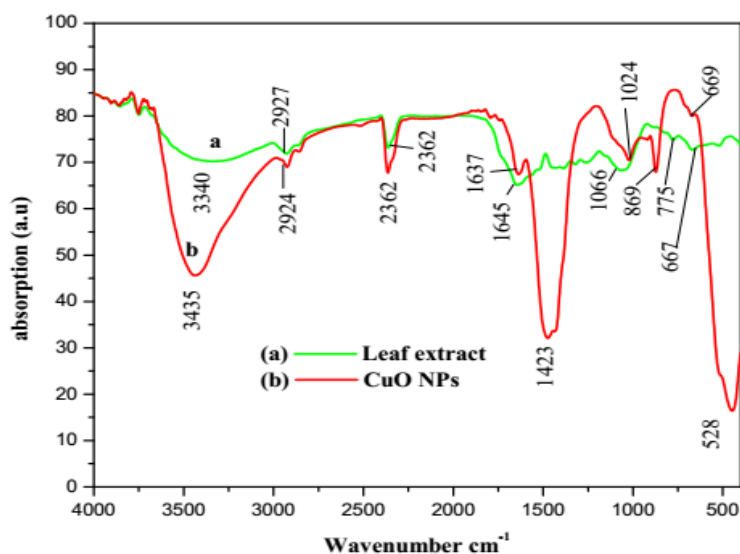


**Figure 4: FT-IR Spectra of (a) Leaf Powder of *Pyrus Pyrifolia* (b) Bio Synthesized CuO Nanoparticles.**<sup>[31]</sup>



### XRD Analysis of CuO NPs

XRD technique is used to realize structural properties of materials and get information like crystal structure/phase, lattice parameters, crystallite size, orientation of single crystals, preferred orientation of poly crystals, defects, strains and so on.<sup>[32]</sup> This technique is suitable for thin films, formal and nano materials. In the case of nanostructures, the change in lattice parameter with respect to bulk gives an idea of the nature of strain present in the film. In XRD, a collimated monochromatic beam of X-rays is incident on the sample for diffraction to occur. A constructive interference occurs only for certain  $\theta$ 's correlating to those planes, where path difference is an integral multiple ( $n$ ) of wavelength. Based on this, the Bragg's condition is given by Equation 2.

$$2d \sin\theta = n\lambda \quad (2)$$

Where,  $\lambda$  is the wavelength of the incident X-ray,  $d$  is the inter-planar distance,  $\theta$  is the scattering angle and  $n$  is an integer-called order of diffraction, In nanostructures, X-rays are diffracted by the oriented crystallites at a particular angle to satisfy the Bragg's condition. Having known the value of  $\theta$  and  $\lambda$  one can calculate the inter-planar spacing. The XRD can be taken in various modes such as  $\theta - 2\theta$  scan mode,  $\theta - 2\theta$  rocking curve, and  $\phi$  scan.

In the  $\theta - 2\theta$  scan mode, a monochromatic beam of X-rays is incident on the sample at an angle of  $\theta$  with the sample surface.<sup>[32]</sup> The detector motion is coupled with the X-ray source in such a way that it always makes an angle  $2\theta$  with the incident direction of the X-ray beam indicating in Figure 5.

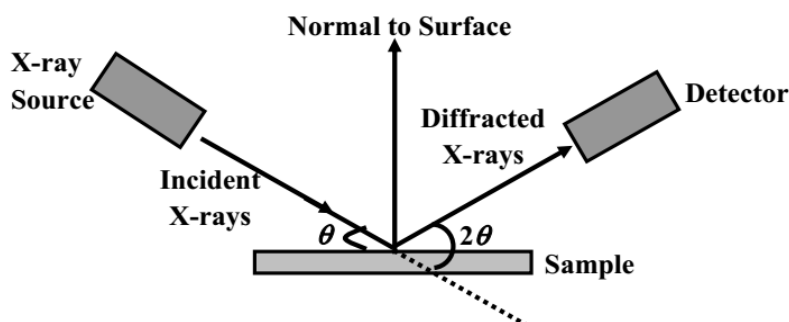


**Figure 5: Schematic Representation on the Working Principles of X-ray Diffraction.**<sup>[30]</sup>

From the XRD pattern, the crystallite sizes of the synthesized CuO nanomaterials by using Cavendish banana peel extract are estimated using Scherere equation 3.<sup>[33]</sup>

$$d = \frac{k\lambda}{\beta \cos\theta} \quad (3)$$

Where,  $d$  is crystallite size in nanometer,  $k$  is shape factor constant, which is 0.89,  $\beta$  is the full width at half maximum (FWHM) in radian,  $\lambda$  is the wave length of the X-ray and  $\theta$  is the Bragg angle. Intensity of XRD spectrum of CuO nanomaterials plotted against  $2\theta$  is shown in Figure 6.

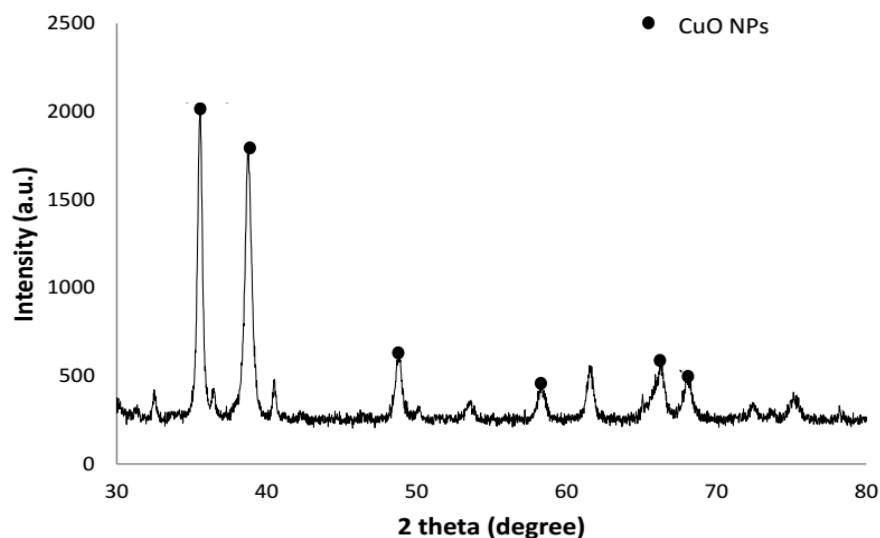


**Figure 6: XRD Pattern of Synthesized CuO NPs from Cavendish Banana Peel Extract.**<sup>[33]</sup>

XRD pattern of CuO NPs displayed that most of the diffraction peaks at  $2\theta$  values  $35.52^\circ$ ,  $38.75^\circ$ ,  $48.76^\circ$ ,  $58.29^\circ$ ,  $66.30^\circ$ ,  $68.02^\circ$ . Similar result was obtained by Wu et al.<sup>[34]</sup> Broadening of the peaks in diffractogram demonstrated that the nanoparticle synthesized was a nanostructure with low crystallinity of 16.1844%. The crystalline size of the CuO NPs was calculated using Debye Scherrer equation. As a result, the crystalline size of CuO NPs corresponds to the highest peak was calculated to be 22.60 nm.<sup>[35]</sup>

### SEM Analysis of CuO NPs

It uses a beam of electrons focused to a diameter spot of approximately 1 nm in diameter on the surface of the specimen and scanned back and forth across the surface (beam energy of 200kV). The surface topography of a specimen is revealed either by the reflected (backscattered) electrons generated or by electrons ejected from the specimen as the incident electrons decelerate secondary electrons. A visual image, corresponding to the signal produced by the interaction between the beam spot and the specimen at each point along each

scan line, is simultaneously built up on the face of a cathode ray tube similar to the manner by which a television picture is generated. The best spatial resolution currently achieved is of the order of 1 nm.<sup>[33]</sup>

The SEM is a very useful instrument to get information about topography, morphology and composition information of materials. It is a type of electron microscope capable of producing high resolution images of a sample surface. Due to the manner in which the image is created, SEM images have a characteristic three-dimensional appearance and are useful for judging the surface morphology of the sample.<sup>[33]</sup>

The SEM has an ability to image a comparatively large area of a specimen and also to image bulk materials. The morphology of the prepared nanoparticles was examined using scanning electron microscopy. Figure 8 shows the surface morphology of the copper oxide nanoparticles. SEM image showed individual copper oxide particles as well as a number of aggregates. The SEM image showed most of the nanoparticles is spherical in shape.<sup>[34]</sup>

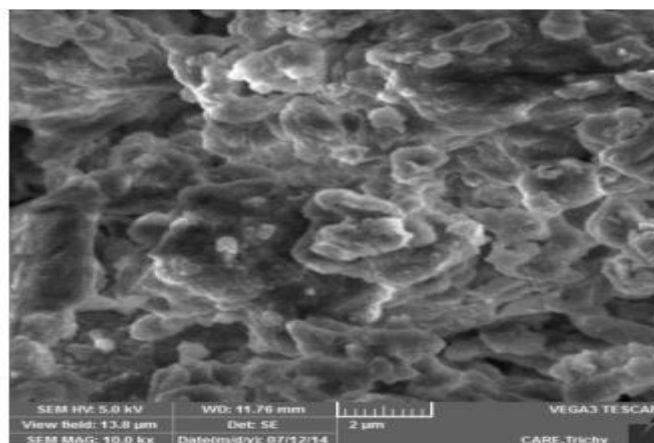


**Figure 7: SEM Image of the Synthesized Copper Oxide Nanoparticles by Using Cavendish Banana Peel Extract.**<sup>[34]</sup>

### Dye Sensitized Solar Cells (DSSCs)

DSSC was first invented by Brian ÓRegan and M.Grätzel. DSSCs are generation of photovoltaic (solar) cell that converts any light energy into electrical energy. The manufacturing cost of DSSCs is approximately 1/3 to 1/5 times that of silicon solar cells.<sup>[35]</sup>

The nano crystalline material plays an essential role in determining the performance of DSSCs in relation to electron injection and transport. The overall conversion efficiency of DSSCs was reported to be proportional to the injection of electrons in to the conduction band

of nanostructure semiconductors. To date, the certified efficiency record is approximately 11.1% for a small cell, and large-scale tests are showing that there is indication for the commercialization of DSSCs.<sup>[36]</sup>

An important feature of the DSSC is the mesoporous semiconductor layer that gives a high surface area. This mesoporosity increases the light harvesting efficiency (LHE) of the cell. However a planar surface covered with a monolayer of a strongly adsorbing sensitizer cannot absorb more than 1% of the light. DSSCs show a very promising future in the field of photovoltaic cells.<sup>[37]</sup>

### **DSSCs Basic Principles and Fundamentals**

In DSSCs, the basic principle of photovoltaic relies on the visible photo-excitation of dye molecules. Upon light absorption by the dye, electrons are excited from HOMO level to LUMO level. The excited electrons from LUMO of dye are transferred to the conduction band of TiO<sub>2</sub> photo electrode. The electrons lost by the dye due to the light absorption are quickly replaced by iodide (I<sup>-</sup>) in the electrolyte solution, which acts as a mediator. The I<sup>-</sup> or triiodide (I<sub>3</sub><sup>-</sup>) results from the oxidized mediator, producing an electron catalyst-coated counter electrode after the electron flows through the load.<sup>[29]</sup> To achieve a reset system capable of repeating the process, energy propagates from the photon to the excited dye photon and then to the TiO<sub>2</sub> layer, conductive glass, load counter electrode I<sup>-</sup>, I<sub>3</sub><sup>-</sup>, and finally to the original TiO<sub>2</sub> location.<sup>[38]</sup> Hence, the electric power generated in DSSCs causes no permanent chemical transformations and is theoretically stable.<sup>[39]</sup> Figure 8 shows the fundamental and basic principles of DSSCs.

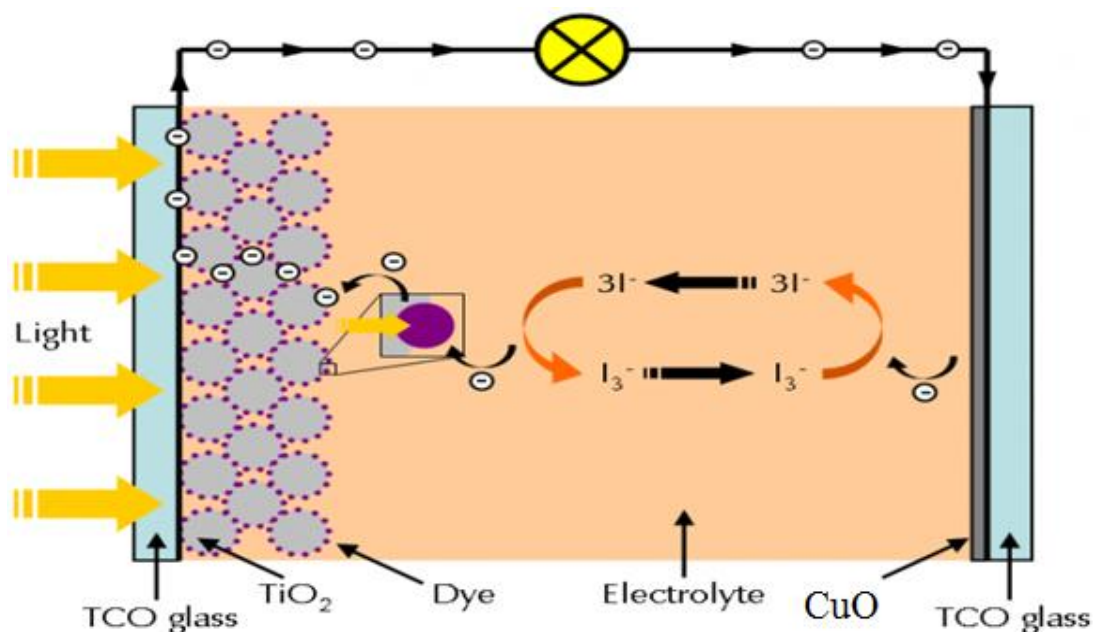


Figure 8: Working Principles of DSSC.<sup>[38]</sup>

## Components of DSSCs

### Transparent Conductive Substrates

Conductive substrates must be highly transparent (transparency > 80%) to allow the maximum passage of sunlight to the active surface area.<sup>[40]</sup> Typically, DSSCs are constructed with two sheets of transparent conductive materials as current collectors for the deposition of the semiconductor and catalyst. The transparent conductive oxide material characteristics determine the efficiency of DSSCs due to the efficient charge transfer of electrical conductivity to minimize energy losses. Fluorine doped tin oxide (FTO,  $\text{SnO}_2:\text{F}$ ) and indium doped tin oxide (ITO,  $\text{In}_2\text{O}_3:\text{Sn}$ ) are typical conductive oxide substrates consisting of soda lime glass coated with FTO or ITO, respectively. The transmittance of ITO films is over 80% in the visible region, with a sheet resistance of approximately ( $18 \Omega \text{ cm}^{-2}$ ), whereas FTO films exhibit a transmittance of approximately 75% with a sheet resistance of  $8.5 \Omega \text{ cm}^{-2}$ .<sup>[40]</sup>

### Dye Sensitizers

Natural dyes are suitable alternative photosensitizers for DSSCs. An efficient solar cell sensitizer should adsorb strongly to the surface of the semiconductor oxide via anchoring groups, exhibit intense absorption in the visible part of the spectrum, and possess an appropriate energy level alignment of the dye excited state and the conduction band edge of the semiconductor. The performance of DSSCs mainly depends on the molecular structure of the photosensitization. Sensitization of the semiconductor in DSSCs has been achieved using

numerous chemical compounds, such as phthalocyanines, coumarin, carboxylated derivatives of anthracene and porphyrins.<sup>[41]</sup> However, the best photosensitization has been attained using metal transition mater. Three classes of dye sensitizers are used in DSSCs: metal complex sensitizers, metal-free organic sensitizers and natural sensitizers. Some of the requirements that an efficient dye sensitizer has to fulfill are: broad and strong absorption, preferably extending from the visible to the near infrared region; minimal deactivation of its excited state through the emission of light or heat; Irreversible adsorption (chemisorption) to the surface of the semiconductor, and a strong electronic coupling between its excited state and the semiconductor conduction band; Chemical stability in the ground as well as in the excited and oxidized states, so that the resulting DSSCs will be stable over many years of exposure to sun light.<sup>[42]</sup>

### Semiconductor Film Electrodes

The semiconductor structure has a thousand times surface area available for dye chemisorption than that of a flat and unstructured electrode of the same size. If the dye is chemisorbed as a monomolecular layer, enough can be retained on a given area of electrode to provide absorption of essentially all the incident light. The need for DSSCs to absorb far more of the incident light is the driving force for the development of mesoporic semiconductor material (minutely structured materials with an enormous internal surface area). Photo electrodes are made of materials such as silicon and cadmium sulfide decomposes under irradiance in solution owing to photo corrosion. In contrast, oxide semiconductor materials, especially  $\text{TiO}_2$ , have good chemical stability under visible irradiation in solution.<sup>[43]</sup> It has been found that  $\text{TiO}_2$  is a stable photo electrode in photo electrochemical systems even under extreme operating conditions. It is cheap, readily available and non-toxic nanoparticle. Its conduction band edge Coincides well with the excited electronic level of anthocyanin containing dyes which is an important condition to be satisfied for the injection of electrons from the dye molecule to the semiconductor.<sup>[44]</sup>

### Redox Couple Electrolyte

Redox couple electrolyte containing  $\text{I}^-/\text{I}_3^-$  redox ions is used in DSSCs to regenerate the oxidized dye molecules and hence completing the electric circuit by mediating electrons between the nano structured electrode and counter electrode. The redox electrolyte needs to be chosen such that the reduction of  $\text{I}_3^-$  ions by injection of electrons is fast and efficient. This arise from the fact that the dependence of both hole transport and collection efficiency on the

dye cation reduction and  $I^-/I_3^-$  redox efficiency at counter electrodes are to be taken into account.<sup>[45]</sup> A redox couple is the key component in a liquid electrolyte, assuming the tasks for dye regeneration and charge transport between the two electrodes, playing a crucial role in determining the photovoltaic performance of DSSCs. An “ideal” redox couple should essentially fulfill certain requirements as follows; the redox potential of a redox couple should be less negative than the oxidized level of a dye molecule, slow electron recombination kinetics at the interface; negligible visible light absorption; fast electron transfer kinetics at CEs; good diffusion properties to avoid mass transport limitations particularly under higher levels of irradiation; non corrosiveness towards collecting metals, and then good photochemical stability. Following the invention of low-cost dye-sensitized solar cells (DSSCs), redox-couple solid electrolytes have attracted considerable attention in recent years. These electrolytes eliminate the short coming of the liquid/gel electrolytes, such as leakage/evaporation of organic solvent especially at elevated temperatures, electrode corrosion, a need of hermetic sealing, and scale up of the manufacturing process.<sup>[46]</sup>

### **Fabrication of DSSCs**

One of the reason, DSSCs has been attracting considerable attention than the other energy source is, because of their simple fabrication process. The fabrication process of dye-sensitized solar cells involves different types of components in order to accomplish the whole assembly.<sup>[40]</sup> The fabrication process of DSSCs involves coating of transparent and conducting oxide (TCO) such as FTO and ITO on a glass substrate. TCO coated substrate is cleaned with some organic solvents such as ethanol, acetone and Isopropanol sequentially using ultrasonicator. Solid  $TiO_2$  is dissolved by appropriate polar solvent in order to prepare pastes of nano materials. The paste of  $TiO_2$  is deposited on to the top of TCO substrate using Doctor Blade technique. The TCO substrates coated with  $TiO_2$  are treated with heat to remove solvent and improve conductivity; and then sensitizers or dyes are deposited on top of  $TiO_2$  photo electrode. The solar cells fabrication is completed after mounting counter electrode on top of sensitized photoelectrodes.<sup>[40]</sup>

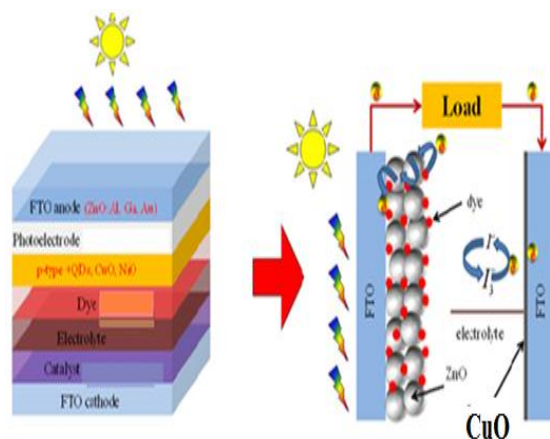


**Figure 1: Schematic Representation of DSSCs Presenting the Structure and Mechanism.**<sup>[40]</sup>

## Characterization of DSSC Devices

### Current-Voltage Characteristics

One of the most essential measurements of DSSCs is the current-voltage (I-V) measurement technique. During illumination of the solar cells at 25<sup>0</sup>C a voltage is applied and the current is measured, resulting in the I-V curve of the cell.<sup>[42]</sup> The I-V characteristics are measured under an external potential between the working electrodes and counter electrode. The three parameters  $J_{SC}$  (the maximum current that can run through the cell is determined by the short-circuit current),  $V_{OC}$  (is the maximum voltage attainable in a solar energy conversion device), and FF (is a measure of the maximum work obtainable from a solar cell with reference to a hypothetical maximum power) can be extracted from the I-V curves.<sup>[47]</sup> The external potential is altered from current density at short circuit conditions ( $J_{SC}$ ) to Voltage at open circuit conditions ( $V_{OC}$ ) or opposite depending on scanning direction. The amount of dye adsorbed on the semiconductor can limit amount of photons get absorbed and then number of electrons injected in to metal oxide electrodes; which in turn limits the short circuit current ( $J_{SC}$ ). In fact, with increasing addition of nano-SnO<sub>2</sub> into ZnO/Fe<sub>2</sub>O<sub>3</sub> mixed oxide, the amount of adsorbed dyes increased, resulting in the increase of  $J_{SC}$  and  $V_{OC}$ .<sup>[47]</sup>

**Open circuit voltage ( $V_{OC}$ ):**-the open circuit photo voltage within the cell is equal to zero. The I-V curve can also be measured under dark conditions. This will give information about recombination to the oxidized redox species. Since no oxidized dye is present in dark, the dark current is a measure of electrons going in the reverse way, from the TiO<sub>2</sub> to the oxidized species of the redox couple. The I-V measurements should be carried out with enough slow



scan rates so the solar cell has time to adjust and no hysteresis effects appear.<sup>[48]</sup> The maximum power point is given by the  $P_{\max}$  ( $P_{MP}$ ) values.

Fill factor is one of the important parameters in order to achieve high efficiency. It is defined as the ratio of the maximum power output ( $P_{MP}$ ) to the product of short circuit photocurrent and open circuit photo voltage, and  $J_{SC}$  and  $V_{OC}$ .

$$FF = \frac{J_{MP} V_{MP}}{J_{sc} V_{oc}} \quad (4)$$

**Power conversion efficiency ( $\eta$ ):**- The overall conversion efficiency ( $\eta$ ) of the dye sensitized solar cell is determined by the photocurrent density ( $J_{SC}$ ), the open-circuit potential ( $V_{OC}$ ), the fill factor (FF) of the cell and the intensity of the incident light.<sup>[48]</sup> The power conversion efficiency is defined as the ratio of  $P_{MP}$  to the incident radiation power ( $p_{in}$ ) on surface the solar cell.

$$\eta = \frac{P_{MP}}{P_{in}} = \frac{J_{sc} V_{oc} FF}{P_{in}} \quad (5)$$

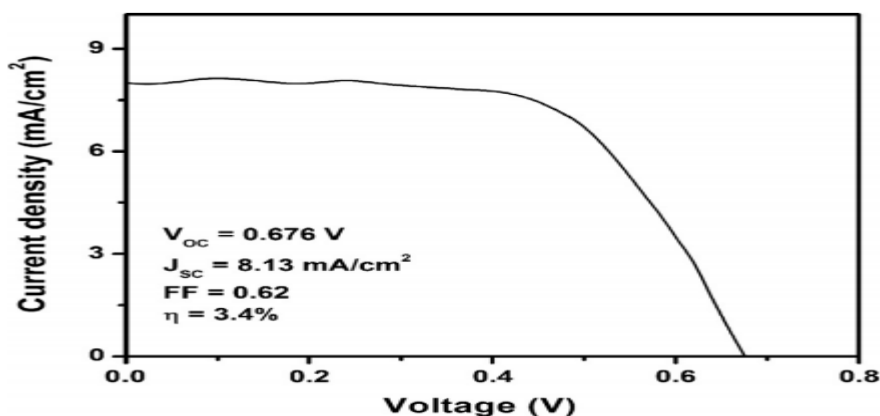


**Figure 2: J–V Curve of DSSC Fabricated with Counter Electrode Based on Synthesized CuO NPs from Leaf of *Calotropis Gigantean*.**<sup>[48]</sup>

### Incident Photon to Current Conversion Efficiency (IPCE)

IPCE sometimes also referred to as quantum efficiency (QE) or external quantum efficiency (EQE) is a measure of how efficient a solar cell is in producing photo-generated charge at a given frequency. High energy conversion efficiency is one of the most important keys to the commercialization of DSSCs in the huge electricity generation.<sup>[49]</sup> The sensitivity of DSSCs varies with the wavelength of the incident light. The IPCE is a measure of the efficiency of the solar cell to convert the incoming photons to photocurrent at different wavelengths. This is done by measuring the resulting photocurrent of the solar cell when illuminated by

monochromatic light.<sup>[50]</sup> The IPCE is a measure of the product of different efficiencies such as light harvesting efficiency (LHE), the quantum yield of electron injection from the excited dye into the TiO<sub>2</sub> conduction band, the efficiency of regeneration  $\eta_{reg}$ , and the collection efficiency of the photo-generated charge carriers'  $\eta_{coll}$ .

$$IPCE = LHE \times \phi_{inj} \times \eta_{reg} \times \eta_{coll} \quad (6)$$

Where LHE is light harvesting efficiency for photons,  $\phi_{inj}$  is electron injection quantum yield for the excited sensitizer to the semi-conductor oxide conduction band and  $\eta_{coll}$  is the fabrication injected charges that is able to the back contact.

IPCE measurement is also useful for indirect determination of the short circuit photocurrent of DSSCs. Percent IPCE can be calculated according to the equation given below.<sup>[49]</sup>

Figure 12 shows the IPCE spectra as a function of the wavelength for TiO<sub>2</sub> sensitized with Isobutrin. It was calculated from the equation:

$$IPCE(\%) = \frac{1240 J_{sc}}{\lambda P_{in}} \times 100\% \quad (7)$$

Where  $J_{sc}$  is the short-circuit current density,  $\lambda$  is the wavelength of the incident light, and  $P_{in}$  is the power of the incident light.

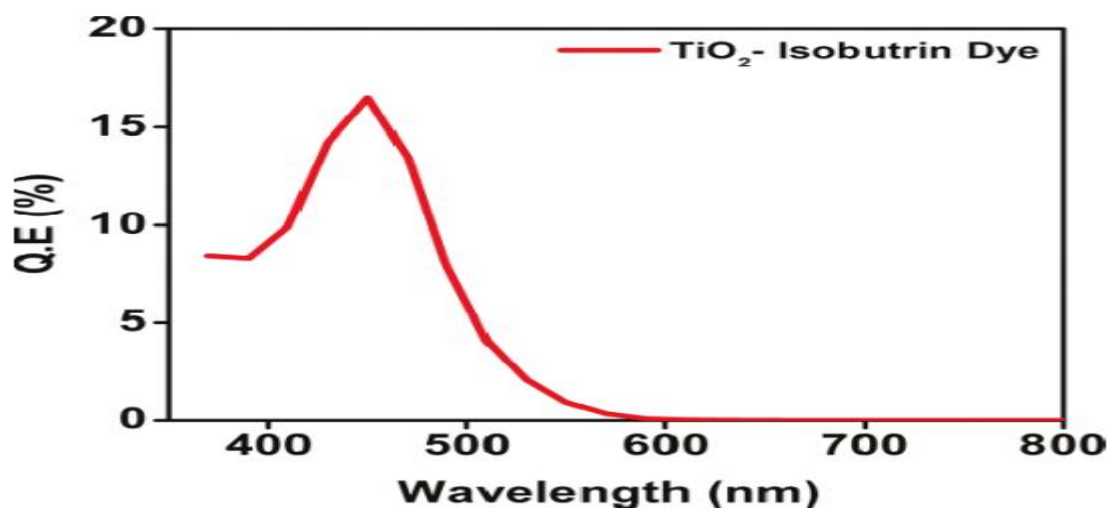


Figure 3: IPCE measurement of isobutrin dye-loaded TiO<sub>2</sub> film.<sup>[49]</sup>

### CuO Nanoparticle for DSSC Application

Among the oxides of transition metals, CuO NPs are of special interest. CuO is a semiconducting material with a narrow band gap and used for photoconductive and photo thermal applications.<sup>[50]</sup> CuO NPs is one of the thin films that can easily be deposited on

substrates using a simple technique. The first photovoltaic cells observed by Becquerel in 1839 used CuO coated metal electrodes immersed in an electrolyte solution. CuO is an inexpensive and non-toxic semiconducting material.<sup>[51]</sup> It is a p-type semiconductor with a narrow band gap (1.2-1.9 eV), which has interesting photovoltaic, electrochemical and catalytic properties. Likewise, studies have reported the doping of TiO<sub>2</sub> for use in DSSCs; can lead to improvements in some of the photovoltaic properties of the cells. Wang and Teng enhanced electron transport in cells doped with zinc under low-intensity illumination. CuO NPs are employed as electro catalytic materials for the fabrication of counter electrode in DSSCs.<sup>[52]</sup>

J. Wu *et al.* reported that CuO NPs from leaf of *Calotropis gigantea* based counter electrode exhibited reasonably good surface for the electrocatalytic activity toward the reduction of I<sub>3</sub> to I<sup>-</sup> ions in redox electrolyte, as obtained the good reduction current.<sup>[47]</sup> Moderately high solar to electrical energy conversion efficiency ~3.4% along with high short circuit current density (J<sub>SC</sub>) of 8.13 mA/cm<sup>2</sup>, open circuit voltage (V<sub>OC</sub>) of ~ 0.676 V and fill factor (FF) of ~ 0.62 is recorded in the DSSC fabricated with synthesized CuO NPs based counter electrode. Therefore, the green synthesis of CuO NPs from the leaves of *C. gigantea* plant could be a promising, low cost & ecofriendly method without using any toxic chemicals. The biosynthesized CuO NPs are applied for the fabrication of efficient DSSC with high photocurrent density and high performance.<sup>[47]</sup>

## CONCLUSION

The green chemistry approach using for the synthesis of CuO NPs is simple, cost effective and the resultant nanoparticles are highly stable and reproducible. The prepared CuO NPs are characterized using XRD, UV-Vis absorption, Raman Spectroscopy, FT-IR, SEM-EDX and TEM techniques. Synthesized CuO NPs is utilized as electrocatalytic materials for the preparation of counter electrode in DSSCs and also used for other applications.

## REFERENCES

1. R. Kubo, A. Kawabata, S. Kobayashi (2012). Electronic properties of small particles. *Annu. Rev. Mater. Sci.*, 19: 682.
2. A.S. Edelstein, (1999). *Nanomaterials: Synthesis, Properties and Applications*, 2<sup>nd</sup> ed., Naval Research Laboratory, 10, 73 Washington, DC.
3. K.P. Jayadevan, T.Y. Tseng, (2004). *Encyclopedia of Nanoscience and Nanotechnology*, H.S. Nalwa, 2nd ed., 8: 4, *American Scientific, California*.

4. A. Rahman, A. Ismail, D. Jumbianti, H. Sudrajat, S. Magdalena (2009). Synthesis of copper oxide nanoparticles by using *Phoridium cyanibacterium*. *J. Chem.*, 9: 355.
5. Y. Zhou, W. Lin, J. Huang, W. Wang, and Y. Gao (2010). Biosynthesis of Gold Nanoparticles by Foliar Broths: Roles of Biocompounds and Other Attributes of the Extracts. *Nanoscale. Res. Lett.*, 5: 1351.
6. V. V. Makarov, A. J. Love, O. V. Sinitsyna, S. S. Makarova, I. V. Yaminsky, M. E. Taliansky, and N. O. Kalinina (2014). "Green" nanotechnologies: synthesis of metal nanoparticles using plants. *Acta Naturae.*, 6: 35.
7. V. Oxana, B. I. Kharissova, C. M. Kharisov and G. Oliva (2019). Greener synthesis of chemical compounds and materials. *J. Royal Soci.*, 6: 15.
8. H. S. Devi and T. D. Singh (2014). Synthesis of copper oxide nanoparticles by a novel method and its application in the degradation of methyl orange. *Adv. Electron. Elect. Eng.*, 4: 83.
9. R. Prasad (2014). Synthesis of Silver Nanoparticles in Photosynthetic Plants. *J. Nanopart.*, 2014: 1.
10. E. W. Wilde and J. R. Benemann (1993). Bioremoval of heavy metals by the use of microalgae. *Biotech. Adv.*, 11: 781.
11. P. Rauwel, S. Kuunal, S. Ferdov and E. Rauwel (2015). A review on the green synthesis of silver nanoparticles and their morphologies studied via TEM advances. *Mat. Sci. Eng.*, 749: 1.
12. G. Singaravelu, J.S. Arokiamary, V.G. Kumar and K. Govindaraju (2007). A novel extracellular synthesis of monodisperse gold nanoparticles using marine alga. *Colloids Surfaces B. Biointerfaces*, 57: 97.
13. Y. Abboud, T. Saffaj, A. Chagraoui, A.E. Bouari, K. Brouzi, O. Tanane and B. Ihssane (2014). Biosynthesis, characterization and antimicrobial activity of copper oxide nanoparticles produced using brown alga extract (*Bifurcaria bifurcata*). *App. Nanosci.*, 4: 571.
14. A. Ingle, A. Gade, S. Pierrat, C. Sonnichsen, MK. Raj (2008). Synthesis of silver nanoparticles using the fungus *Fusarium acuminatum* and its activity against some human pathogenic bacteria. *Curr Nanosci.*, 4: 141.
15. D. R. Majumder (2012). "Bioremediation: copper nanoparticles from electronic-waste." *Int. J. Eng. Sci. Techno.*, 4: 4380.

16. S. Honary, H. Barabadi, E. Gharaei-Fathabad, and F. Naghibi (2012). "Green synthesis of copper oxide nanoparticles using *Penicillium aurantiogriseum*, *Penicillium citrinum* and *Penicillium waksmani*." *Dig J Nanomater Biostruct.*, 7: 999.
17. C. Noguez (2007). "Surface plasmons on metal nanoparticles: the influence of shape and physical environment." *J. Phys. Chem.*, 111: 3606.
18. H.-J. Lee, J. Y. Song and B. S. Kim (2013). "Biological synthesis of copper nanoparticles using *Magnolia kobus* leaf extract and their antibacterial activity," *J. Chem. Technol. Biotechnol.*, 88: 1971.
19. E. Bäuerlein, *Angew* (2003). Bomineralization of Unicellular Organisms: An Unusual Membrane Biochemistry for the Production of Inorganic Nano and Microstructures. *Chem. Int. Ed.*, 42: 614.
20. R. Usha, E. Prabu, M. Palaniswamy, C. K Veni, K. R Rajendran (2010). Synthesis of metal oxide nanoparticles by *Sterptomyces* species for development of antimicrobial textiles. *J. Biotechno. Biochem*, 5: 153.
21. D. Mandal, M. E Bolander, D. Mukhopadhyay, G. Sarkar, P. Mukherjee (2006). The use of microorganisms for the formation of metal nano particles and their application. *Microbiol. Biotechnol.*, 69: 485.
22. S. Baker, D. Rakshith, K. S. Kavitha, P. Santosh, H. U. Kavitha, Y. Rao, and S. Satish (2013). Plants emerging as nanoparticles towards facile route in synthesis of nanoparticles. *BioImpacts*, 3: 111.
23. J. Sen, P. Prakash, and N. De (2015). Nano clay composite and phytonanotechnology: a new horizon to food security issue in Indian agriculture. *J. Glob. Biosci.*, 2: 187.
24. H. R. Naika, K. Lingaraju, K. Manjunath, D. Kumar, G. Nagaraju, D. Suresh, and H. Nagabhushana (2015). Green synthesis of CuO nanoparticles using *Gloriosa superba* L. extract and their antibacterial activity. *J. Taibah. Univ. Sci.*, 9: 7.
25. Jayalakshmi and A. Yogamoorthi (2014). Green synthesis of copper oxide nanoparticles using aqueous extract of flowers of *Cassia alata* and particles characterization. *Int. J. Nanomater. Biostruct.*, 4: 66.
26. W. Yunfang, L. Xiuli, W. Yawen and F. Caimei (2013). Novel visible-light AgBr/Ag<sub>3</sub>PO<sub>4</sub> hybrids photocatalysts with surface plasma resonance effects. *J. Solid State Chem.*, 202: 51.
27. C. Kusumawardani, K. Indriana, Narsito (2010). Synthesis of Nanocrystalline N-Doped TiO<sub>2</sub> and Its Application on High Efficiency of Dye-Sensitized Solar Cells. *J. Sci.*, 1: 1.

28. J. Xia, H. Li, Z. Luo, H. Shi, K. Wang, H. Shu, Y. Yan (2009). Facile Synthesis of Mesoporous CuO Nanoribbons for Electrochemical Capacitors Applications *J. Phys. Chem.*, 70: 1461.
29. H. R. Ghorbani, I. Fazeli, A. A. Fallahi (2015). A Biological Approach for the Synthesis of Copper Oxide Nanoparticles by *Ixora Coccinea* Leaf Extract. *Orient. J. Chem.*, 31: 515.
30. M. K. Nazeeruddin, E. Barano, and M. Grätzel (2011). Molecular interaction and charge transfer of triphenylamine-based dye on rutile TiO<sub>2</sub>. *J. Chem. Phys.*, 85: 1172.
31. V. Vellora, T. Padil, and M. Černík (2013). Green synthesis of copper oxide nanoparticles using gum karaya as a biotemplate and their antibacterial application. *Int. J. Nanomed.*, 8: 889.
32. G. Thomas, (1972). *Transmission Electron Microscopy of Metals*, John Wiley & Sons Inc., 34: 274, New York, London.
33. X. Z. Li (2004). Simulation of polycrystalline electron diffraction pattern and phase identification. *ultramicroscopy*, 99: 257.
34. R. Wu, Z. Ma, Z. Gu, and Y. Yang (2010). Preparation and characterization of CuO nanoparticles with different morphology through a simple quickprecipitation method in DMAC water mixed solvent. *J. Alloys. Compd.*, 504: 45.
35. A. N. S. Rao, and V. T. Venkatarangaiiah (2014). The effect of ceyltrimethylammonium bromide on size and morphology of ZnO and CuO. *J. Electrochem. Sci. Eng.*, 4: 97.
36. <http://www.chemistryexplained.com/Ru-Sp/Solar-Cells.html>.
37. A. H. Reshak, M. M. Shahimin, N. Juhari, R. Vairavan (2013). Photovoltaic characteristics of hybrid MEH-PPV-nanoparticles compound. *Cur. App. Phy.*, 13: 1.
38. A. V. S. Reddy, I. A. Hussein, K. Harrabi, U. Mehmood, S.U. Rahman (2014). Enhancing Power Conversion Efficiency of Dye Sensitized Solar cell using TiO<sub>2</sub> composite Photoanodes. *Adv. Mater. sci. eng.*, 2014: 1.
39. A. Sima, C. Grigoriu, S. Antohe (2010). Materials for Enhanced Dye-sensitized Solar Cell Performance, Electrochemical Application *Inorg. Chem.*, 519: 595.
40. J. Gong, J. Liang, K. Sumathy (2012). Review on dye sensitized solar cells (DSSCs) fundamental concepts and novel materials, Renew and Sustain Energy Review. *Inorg Chem.*, 16: 5848.
41. A. Olea, G. Ponce, P. J. Sebastian (1999). Evaluation of Anthocyanin, a Rose Residue Extract, for Use in Dye-Sensitized Solar Cell. *Sol. Energ. Mat. Sol. Cells.*, 59: 137.

42. S. Yanagida, C. R. Chemie (2006). Application of Hibiscus Sabdariffa and leaves of Azardirachta Indica calyxes as sensitizers in Dyesensitized solar cells. *Int. J. Eng. Res. Dev.*, 9: 597.
43. M. Matsumoto, Y. Wada (2001). Nanostructured Materials for Solar Energy Conversion. *Bull. Chem. Soc. Japan.*, 174: 387.
44. B. Ghorpade, M. Darvekar, P.S. Vankar, (2000) Ecofriendly cotton dyeing with Sappan wood dye using ultrasound energy. *Colourage*, 47: 27.
45. L. G. Hubert-Pfalzgraf, S. Daniele, J.M. Decams (2003). Novel synthesis and applications of functional carbon, transition metal oxides and their nanocomposites. *J. Sol-Gel Sci. Technol.*, 11: 1.
46. Y. Chiba, A. Islam, Y. Watanabe, R. Komiya, N. Koide, L. Y. Han (2006). Dye-Sensitized Solar Cells with Conversion Efficiency of 11.1%. *J. Appl. Phys.*, 45: 24.
47. J. Wu, Q. Li, L. Fan, Z. Lan, P. Li, J. Lin, S. Hao (2008). High-performance polypyrrole nanoparticles counter electrode for dye-sensitized solar cells. *J. Power. Sources*, 181: 172.
48. J. P. Vahermaa, K. Miettunen, P. Lund (2010). Interface electric properties of Si/organic hybrid solar cells using impedance spectroscopy analysis. *Adv. Mate.*, 22: 221.
49. J. Halme, P. Vahermaa, K. Miettunen, and P. Lund (2010). Charge transport and photocurrent generation characteristics in dye solar cells containing thermally degraded N719 dye molecules. *Adv. Mate*, 22: 210.
50. D.U. Onah, E.I. Ugwu, J.E. Ekpe (2015). Optical characteristics of CuO thin film prepared by Chemical spray pyrolysis. *J. nano.*, 3: 62.
51. K. Wang, H. Teng (2009). Electronic Supplementary Information. *J. Mat. Chem.*, 55: 1.
52. M. Grätzel (2001). Photoelectrochemical cells. *Nature*, 414: 338.